

NASA
Technical Memorandum 102360

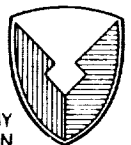
AVSCOM
Technical Report 89-C-018

Oxidation Effects on the Mechanical Properties of SiC Fiber-Reinforced Reaction-Bonded Silicon Nitride Matrix Composites

Ramakrishna T. Bhatt
Propulsion Directorate
U.S. Army Aviation Research and Technology Activity—AVSCOM
Lewis Research Center
Cleveland, Ohio

November 1989

NASA

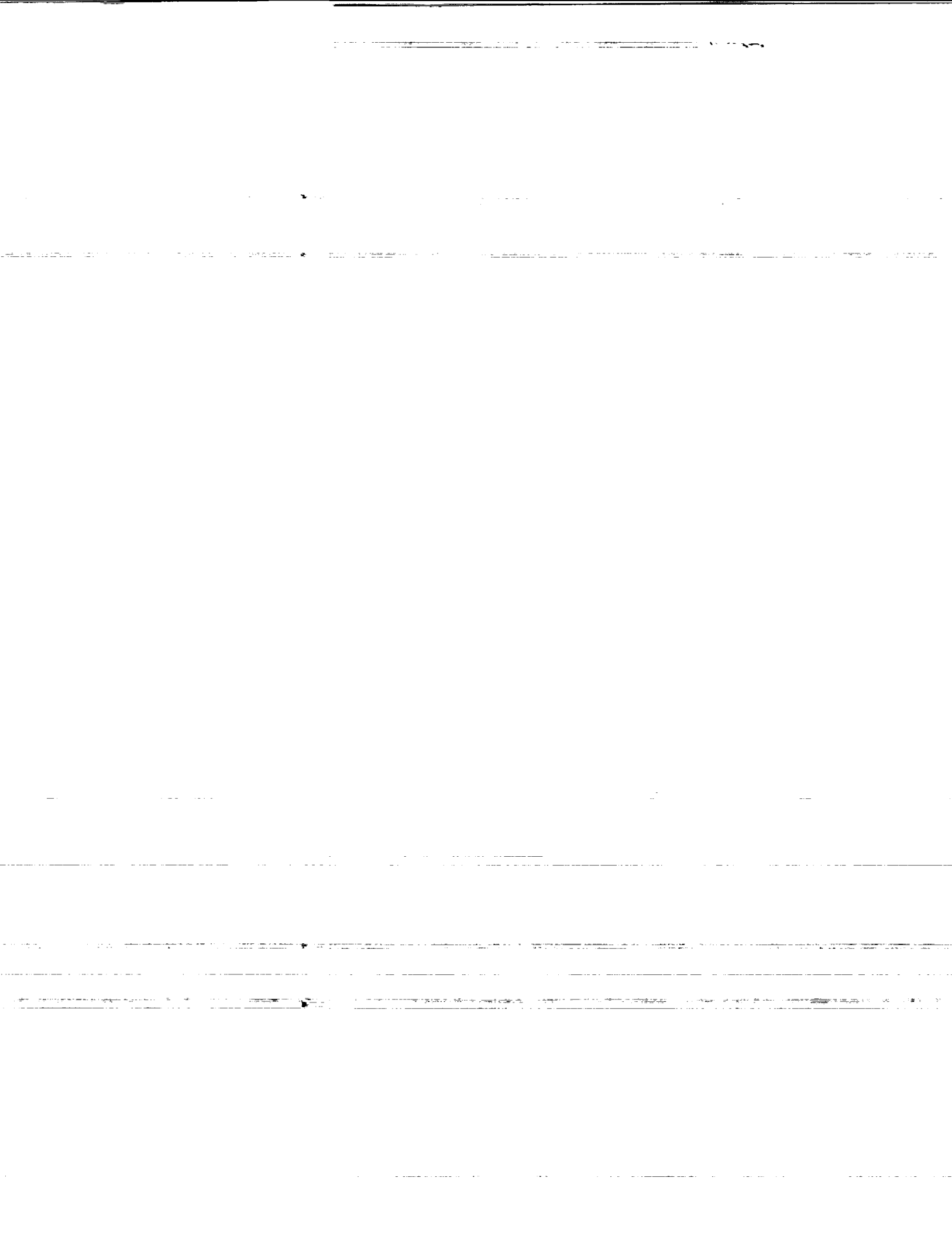


US ARMY
AVIATION
SYSTEMS COMMAND
AVIATION R&T ACTIVITY

(NASA-TM-102360) OXIDATION EFFECTS ON THE
MECHANICAL PROPERTIES OF SiC
FIBER-REINFORCED REACTION-BONDED SILICON
NITRIDE MATRIX COMPOSITES (NASA) 38 p

N90-14287

Unclass
CSCL 11D G3/24 0243204



OXIDATION EFFECTS ON THE MECHANICAL PROPERTIES OF SiC FIBER-REINFORCED
REACTION-BONDED SILICON NITRIDE MATRIX COMPOSITES

Ramakrishna T. Bhatt
Propulsion Directorate
U.S. Army Aviation Research and Technology Activity - AVSCOM
Lewis Research Center
Cleveland, Ohio 44135

ABSTRACT

The room temperature mechanical properties of SiC fiber-reinforced reaction-bonded silicon nitride composites (SiC/RBSN) were measured after 100 hr exposure at temperatures to 1400 °C in flowing nitrogen and in oxygen environments. The composites consisted of ~30 vol % uniaxially aligned 142 μm diameter SiC fibers (Textron SCS-6) in a reaction-bonded Si₃N₄ matrix. The results indicate that composites heat-treated in a nitrogen environment at temperatures to 1400 °C showed deformation and fracture behavior equivalent to that of the as-fabricated composites. On the other hand, the composites heat-treated in an oxidizing environment beyond 400 °C yielded significantly lower ultimate tensile strength values. Specifically in the temperature range from 600 to 1000 °C, composites retained ~40 percent of their as-fabricated strength, and those heat-treated in the temperature range from 1200 to 1400 °C retained ~70 percent. Nonetheless for all oxygen heat treatment conditions, composite specimens displayed strain capability beyond the matrix fracture stress; a typical behavior of a tough composite. For the oxygen treated composites, the variation of the primary elastic modulus, the first matrix cracking stress, and the interfacial shear strength with heat treating temperature showed trends similar to that of the ultimate tensile strength. Thermogravimetric and microstructural characterization results indicate that the oxygen effects were influenced by two different reactions, namely

E-5074

oxidation of the carbon-rich fiber surface coating and oxidation of the RBSN matrix. The dominant oxidation reaction controlling mechanical behavior depended on the exposure temperature, that is, the carbon reaction occurring from 600 to 1000 °C and the matrix reaction occurring above 1000 °C. Surface coating the composites with a thin layer of silica by a flash oxidation technique appears to have no significant influence on oxidation effects.

I. INTRODUCTION

For improving the efficiency and performance of current air breathing high performance engines, oxidation and creep resistant materials are required that are lightweight, strong, and tough, and able to withstand high temperature and high heat flux. Although monolithic ceramics are prime candidates for these applications, they are not fully utilized because of their low toughness and brittle catastrophic fracture behavior. On the other hand, fiber-reinforced ceramic matrix composites offer the potential for retaining the useful properties of monolithic ceramics while improving their toughness and failure characteristics.

Several fiber reinforced ceramic matrix composites are currently at different stages of development.¹⁻⁶ One system which shows promise for advanced propulsion components is SiC fiber-reinforced reaction-bonded silicon nitride.^{5,6} In the as-fabricated condition, SiC/RBSN composites display a metallike stress-strain behavior, graceful failure beyond matrix fracture, and strength properties superior to that of unreinforced RBSN of comparable density. In addition, their room temperature tensile properties are relatively independent of tested volume, and are unaffected by artificial notches normal to the loading direction or by thermal shocking from temperatures to 1100 °C.⁵ These improvements in composite properties are obtained because of the use of high modulus, high strength, high purity SiC fibers that did not degrade or react with the matrix to form a strong chemical

bond in the thermal and environmental conditions associated with composite fabrication.

Because of their low density, high strength, and noncatastrophic failure behavior, the SiC/RBSN composites and their advanced modifications show potential for use in high temperature structural components of advanced aerospace engines. However, a major issue is whether the metallike stress-strain behavior and excellent structural properties observed for the composites in the as-fabricated condition can be retained after exposure to thermal and environmental conditions similar to those of high performance engines. A recent study⁵ has indicated that after 15 min exposure in air at temperatures to 1400 °C, this composite retained its as-fabricated strength properties. The objectives of this study were to determine the influence of long term (100 hr) heat treatments in oxygen and nitrogen for temperatures up to 1400 °C on SiC/RBSN properties and to identify any degradation mechanisms that may occur.

II. EXPERIMENTAL

(1) Composite Fabrication

The starting materials for SiC/RBSN composite fabrication were double coated SCS-6 SiC monofilaments* and high purity silicon powder† of average particle size 0.3 μm.

The SCS-6 SiC fibers, produced by chemical vapor deposition of methyl-trichlorosilane onto a heated carbon substrate, have a complex microstructure and can be considered as micro-composites in themselves. A schematic diagram of the cross section of the fiber is shown in Fig. 1(a). The fiber consists essentially of a SiC sheath with an outer diameter of 142 μm surrounding a pyrolytic graphite coated carbon core with diameter of

*Textron Specialty Materials Division, Lowell, Massachusetts.

†Union Carbide, New York, New York.

37 μm . The sheath is comprised entirely of columnar $\beta\text{-SiC}$ grains and contains two zones; the inner zone, referred to as A in Fig. 1(a), contains carbon-rich SiC and the outer zone, referred to as B in the same figure, is essentially stoichiometric SiC. The outer surface of the SiC sheath contains two layers of a carbon-rich coating whose chemical composition verses thickness is shown schematically in Fig. 1(b). This surface coating serves several purposes: it seals off surface flaws on the SiC sheath; it improves the abrasion resistance and handling of the fiber; it serves as sacrificial coating during fabrication of composites; and in some composite systems, it provides the local interfacial microstructural mechanisms needed for matrix crack deflection and for composite toughness.

The composites were consolidated by a conventional ceramic powder fabrication method using a polymer fugitive binder. Figure 2 shows the steps involved in the fabrication. A more detailed description of the composite fabrication is reported elsewhere.⁷ Briefly, the composites were fabricated by a three step process. In the first step, SiC fiber mats and silicon cloth were consolidated with two different polymer fugitive binders - one polymer for maintaining proper spacing between the fibers in the fiber mat and the other polymer for preparing pliable silicon cloth. The volume fraction of fiber in the final composite was controlled by either varying the thickness of the silicon cloth or changing the spacing between fibers in the mat. In the second step, alternate layers of SiC fiber mats and the silicon cloths were stacked in a metal die and pressed in a vacuum hot press under an applied stress from 27 to 2000 MPa for up to 1 hr in the temperature range from 600 to 1000 °C. In the third step, the consolidated SiC/Si preforms were heat-treated in a high purity (>99.99 percent) nitrogen environment in the temperature range from 1000 to 1400 °C for up to 100 hr to convert them to

SiC/RBSN composites. The typical dimensions of the as-nitrided composite panels were 150 by 50 by 2.2 mm.

A representative photomicrograph of the polished cross section of the 30 vol % SiC/RBSN composite specimen is shown in Fig. 3. The composite matrix contained ~30 vol % porosity and displayed density variations around the fibers. The carbon core, the carbon rich surface coatings, and the two zones in the SiC fibers can also be seen in the figure. The average room temperature physical and mechanical properties for the composite are given in Table I.

(2) Specimen Preparation and Testing

The specimens for thermal stability and for thermogravimetric analysis (TGA) were prepared from the composite panels by cutting and grinding them with a diamond impregnated abrasive wheel. Nominal dimensions of the thermal stability and TGA specimens were 127 by 12.7 by 2.0 mm and 25 by 12.7 by 1.2 mm, respectively. For ease of suspending it in the TGA unit, each TGA specimen at one end was provided with a 3 mm hole that was drilled with an ultrasonic diamond particle blaster. After the machining operations, both groups of specimens were thoroughly cleaned in an ultrasonic bath with acetone, dried, and stored in an oven set at 100 °C.

For the thermal stability study, the tensile specimens were directly heat treated in flowing oxygen and in nitrogen for 100 hr at various temperatures to 1400 °C. After cooling to room temperature, these specimens were prepared for tensile tests by adhesively bonding glass fiber reinforced epoxy tabs at their ends leaving 50 mm as the test gauge length. A wire wound strain gauge was adhesively bonded to the specimen gauge section for monitoring axial strains. The tensile specimens were tested at room temperature in an Instron machine at a crosshead speed of 1.3 mm/min. For each heat-treatment condition,

at least five specimens were tested and the average value of the mechanical property data was determined. The fractured specimens were examined using optical and SEM microscopy to determine composite failure behavior.

To determine the effects of similar heat treatment on the fibers, batches of SCS-6 SiC fibers, each containing twenty fibers of length 125 mm, were weighed, heat-treated in nitrogen and in oxygen for 100 hr at 200° intervals in the temperature range from 400 to 1400 °C, cooled to room temperature, and then reweighed. The heat-treated fibers were prepared for tensile testing by forming aluminum foil clamps at each end of the fiber, leaving 50 mm as the gauge length. The aluminum foils were then inserted in pneumatic grips and the fiber specimens were pulled to failure at room temperature using an Instron tensile testing machine at a constant cross head speed of 1.3 mm/min.

For the thermogravimetric analysis (TGA), unreinforced RBSN matrix and SiC/RBSN composites were monitored in a vertically mounted TGA unit. This unit consists essentially of a micro recording balance* mounted above a gas tight alumina reaction tube and a vertical tube furnace which can be translated around the reaction tube. Each TGA specimen was hung on a hook formed at one end of a small diameter alumina rod. A similar hook at the other end of the alumina rod was connected to a platinum wire chain which was suspended from the bottom end of the pan of the micro recording balance into the alumina tube. Commercial grade oxygen gas was passed through the TGA unit at a rate of 100 cc/min in a downward direction. At the beginning of the experiment, the furnace was moved to the bottom end of the alumina tube and heated to the intended temperature. Since the TGA specimen was kept well away from the heated zone, it was heated only up to 200 °C at the maximum furnace temperature of 1400 °C. The temperature in the vicinity of the TGA specimen

*Cahn Instruments, Inc., Cerritos, California.

was recorded using a shielded Pt-Pt+10% Rh thermocouple. After heating the furnace to the desired temperature, it was moved to the region where the TGA specimen was hung. The weight changes occurring in the specimen during isothermal exposure were continuously monitored with the recording microbalance. At least 3 specimens were tested for each exposure condition.

(3) Microstructural Characterization

Polished cross sections of composites were prepared for microstructural analysis by grinding the specimens successively on 40, 30, 15, 10, 6, and 3 μm diamond impregnated metal discs and finally by polishing them in a vibratory polisher on micro cloth using 0.03 μm diamond powder. The polished specimens were ultrasonically cleaned in alcohol, dried, and sputter coated with thin layer of pyrolytic carbon. These specimens were examined in a scanning electron microscope equipped with an energy dispersive x-ray spectrometer (EDAX).

To identify the evolution of new phases, oxidized specimens in bulk and in powdered forms were analyzed by x-ray diffraction (XRD). For this purpose, the specimens were ground in a B_4C mortar and pestle to avoid any contamination. The XRD runs were made at a scanning speed of 1 deg/min using standard equipment with a Ni filter and $\text{Cu K}\alpha$ radiation.

III. RESULTS

(1) Environmental Effects on Mechanical Properties

The room temperature stress-strain curves for the SiC/RBSN composites after 100 hr heat treatment in a nitrogen environment at temperatures to 1400 °C and in oxygen to 400 °C were equivalent to those for the composites in the as-fabricated condition. However, the curves for the composites after heat treatment in oxygen in the temperature range from 600 to 1400 °C were quite different. Typical room temperature stress-strain curves for the

composites in the as-fabricated condition and after heat treatment in oxygen at 400, 600, and 1400 °C for 100 hr are shown in Fig. 4. In general, these stress-strain curves displayed three distinct regions: an initial linear region followed by a nonlinear region and a second linear region. The nonlinear region started with the onset of a through thickness matrix crack normal to the loading direction. The stress corresponding to the deviation from the first linear region is considered as the initial matrix fracture stress. With continued loading, additional matrix cracks were formed at regular intervals along the gauge length. Comparison of the stress-strain curves in Figure 4 shows that the first matrix cracking stress and the slope of the initial linear region for the composites in the as-fabricated condition and after oxygen heat treatment at 400 and 1400 °C were similar, but their ultimate tensile strengths were quite different. In contrast, the composite heat treated at 600 °C showed lower values of primary modulus, first matrix cracking stress, and ultimate composite strength than those for the composites in the as-fabricated condition. Moreover, with continued loading beyond their maximum load carrying capability, the 600 °C specimens showed continuous loss in load with time. This resulted in a long tail to the stress-strain curve.

Examination of fractured tensile specimens by optical and scanning electron microscopy revealed the failure behavior of the composites. The composites in the as-fabricated condition and after oxygen heat treatment at 400 °C fractured in a broom-like manner with very little matrix around the fibers. On the other hand, composites heat treated at 600 °C and at 1000 °C failed with extensive fiber pull out and widely spaced matrix microcracks; whereas those heat treated at 1400 °C fractured with matrix microcracks close to the primary fracture surface and limited fiber pull out. The optical photographs of representative fractured specimens of composites in the as-fabricated condition and after heat treatment in oxygen at 600 and 1400 °C

are shown in Fig. 5. A higher magnification photograph of a fracture surface of a specimen heat treated at 1000 °C (Fig. 6) shows improved bonding between the outer layer of the fiber surface coating and the RBSN matrix, as well as a gap between the fiber inner coating layer of the SiC sheath.

The room temperature stress-strain curves of the as-fabricated and heat-treated composites were employed to evaluate the environmental effects on the primary elastic modulus, the matrix cracking stress, and the ultimate composite tensile strength. The room temperature primary elastic moduli of the composites heat treated in nitrogen and oxygen for 100 hr are shown in Fig. 7 as a function of temperature. These results indicate that the primary modulus values for the composites heat treated in nitrogen in the temperature range from 400 to 1400 °C and for the composites heat treated in oxygen at 400 °C, 1200 and 1400 °C were similar to those for the composites in the as-fabricated condition. However, for those specimens after treatment in oxygen at temperatures beyond 400 °C, initially, the modulus decreased rapidly and then reached a value of 1.2 GPa at 600 °C. From 600 to 1000 °C, the modulus slowly increased, and then reached a value equivalent to that of the as fabricated beyond 1200 °C.

The matrix cracking stress and the ultimate tensile strength as a function of heat-treatment temperature for the composites exposed to nitrogen and to oxygen environments are shown in Fig. 8. Because of the large variation in the ultimate tensile strength measured from batch to batch, the strength data in Fig. 8 are normalized with respect to as-fabricated strength of the control specimen from the same batch. It is apparent from Fig. 8 that the composites heat-treated in the nitrogen environment at temperature to 1400 °C did not show any appreciable loss in strength properties. On the

other hand, composites heat-treated in an oxygen environment at temperatures above 400 °C showed loss in both the first matrix cracking stress and the ultimate tensile strength, but the loss in ultimate tensile strength in the temperature range of 400 to 1200 °C was far greater than the loss of first matrix cracking stress in the same temperature range. In contrast, composites after heat treatment in oxygen at 1200 and 1400 °C retained, respectively, nearly 95 percent and 70 percent of the first matrix cracking stress and ultimate tensile strength values measured for as-fabricated composites.

To determine the influence of long time oxidative exposure at high temperatures on fiber/matrix bond integrity, the interfacial shear strength, τ , was calculated from the Aveston, Cooper and Kelly (ACK) theory⁸ using the matrix crack spacing and the first matrix cracking stress values measured in this study. That is, the interfacial shear strength was estimated from the equation,⁸

$$\tau = \sigma_c^f D_f / (2.98 \times V_f (1 + E_f V_f / E_m V_m)) \quad (1)$$

where σ_c^f is the matrix cracking stress, x is the mean separation between matrix cracks, D_f is the fiber diameter, V_f is the fiber content, and E_f and E_m are elastic moduli of the fiber and the matrix, respectively. The first matrix cracking stress was obtained from the tensile stress-strain curve and the average matrix crack spacing was determined from direct optical measurement. For the latter purpose, the tensile specimens were loaded well beyond the first matrix cracking stress - typically to 75 percent of the average ultimate strength of the composites - and unloaded. The specimen gauge sections were then examined under an optical microscope and the average matrix crack spacing was recorded. The measured values of the first matrix cracking stress and the average matrix crack spacing for the composites in the untreated condition and after heat treatment in an oxidizing environment at temperatures to 1000 °C are shown in Table II.

Substituting $E_f = 390 \text{ GPa}$,⁹ $E_m = 110 \text{ GPa}$,⁵ $D_f = 142 \text{ }\mu\text{m}$, and appropriate values of matrix cracking stress and the matrix crack spacing from Table II in Eq. (1), the interfacial shear strength with heat treatment temperature was calculated. The results plotted in Fig. 9 indicate that up to 400 °C interfacial shear strength values for the heat treated composites were the same as that for the as-fabricated composites, but with increasing exposure temperature, shear strength decreased drastically and reached a value of 0.8 MPa from 600 to 1000 °C.

For composites heat treated in oxygen at 1200 and 1400 °C, the matrix micro cracks were seen very close to the primary fracture surfaces. This behavior is quite different from the regular matrix micro cracking behavior observed in composite specimens that were heat treated at temperatures less than 1200 °C or in the as-fabricated condition when stressed above the first matrix cracking stress. Therefore, no attempt was made to estimate the interfacial shear strength for these composites.

(2) Environmental Effects on SiC Fibers

To determine their environmental stability, as-received SCS-6 SiC fibers were weighed first and then exposed to oxygen and nitrogen environments for 100 hr at temperatures to 1400 °C. After exposure the fibers were weighed again and tensile tested at room temperature. The weight changes measured for the fibers are shown in Fig. 10 for the temperature range from 400 to 1400 °C. Figure 10 shows that fibers heat treated in nitrogen to 1400 °C or in oxygen up to 400 °C showed no apparent change in weight. However, fibers heat-treated in oxygen beyond 400 °C indicated increased weight loss with increasing exposure temperature up to 900 °C and then the trend reversed. At 1400 °C, the fibers showed only a small weight loss.

The room temperature tensile strength for the SCS-6 SiC fibers after heat treatment in nitrogen and in oxygen for 100 hr at temperatures to 1400 °C are

shown in Fig. 11. Included in the figure is the tensile strength value for the untreated SiC fibers. Each data point is an average of 20 individual fiber strength measurements. The error bars represent two standard deviations. Figure 11 indicates that the tensile strength of fibers heat treated in nitrogen at temperatures to 1000 °C was ~3.75 GPa which is equivalent to that of the fibers in as-fabricated condition, but those heat treated at 1200 °C and at 1400 °C showed ~10 and 50 percent lower values. On the other hand, fibers exposed to an oxygen environment at 400 °C showed strength values similar to as-fabricated fibers, but those heat treated in the temperature range of 600 to 1400 °C showed strength loss; the higher the exposure temperature, the lower the ultimate tensile strength.

Microstructural examination of tensile fracture surfaces of oxygen treated SCS-6 SiC fibers showed evidence of surface coating degradation after 100 hr exposure at elevated temperatures. Up to 400 °C, the carbon-rich coating was stable. However, beyond 400 °C increasing amounts of carbon-rich surface coating were oxidized with increasing exposure temperature. As a result, a small decrease in fiber diameter as well as oxide growth at the fiber surface was noticed. Typical photographs of secondary electron and the elemental x-ray images of carbon and oxygen for the untreated and oxygen treated fiber at 600 °C for 100 hr are shown in Fig. 12. Below 1200 °C, XRD analysis showed that this oxide was amorphous, but above 1200 °C it was crystalline cristobalite.

(3) Thermogravimetric Analysis

The kinetics of oxidation for the unreinforced RBSN and SiC/RBSN composites were monitored with thermogravimetry. Isothermal oxidation curves were generated at 200 °C increments from 400 to 1200 °C for up to 100 hr. The oxidation curves for the monolithic RBSN and the SiC/RBSN composites are

243204

N90-14287

Unclas

(NASA-TM-102360) OXIDATION EFFECTS ON THE MECHANICAL PROPERTIES
OF SiC FIBER-REINFORCED REACTION-BONDED ...
(NASA) Nov. 1989 38 p
NAS 1.15:102360 ... Ramakrishna T. Bhatt

G3
C
24

in Figs. 13 and 14, respectively. Data were plotted as percent weight gain rather than weight change per unit area because oxidation occurred internally as well as at the surface. Comparison of the figures indicates that at the same temperature of exposure, the general shape of the oxidation curves for the monolithic RBSN and the composite were similar. At 400 and 600 °C, oxidation curves for RBSN showed two regions: an initial weight loss region where specimen weight decreased rapidly with exposure time, and a second region where specimen weight remained relatively constant. At 800 °C, (for composites at 1000 °C) the oxidation curves generally displayed three regions; an initial weight loss region accompanied by a rapid weight gain region and finally a slow weight gain region. The initial weight loss region for the monolithic RBSN usually lasted for only 10 min, but for the composite it prevailed up to 3 hr depending on the exposure temperature. For a better representation, this region for the monolithic and the composites in the temperature range from 800 to 1400 °C is shown separately at the left in Figs. 13 and 14.

Monolithic and composite specimens after 100 hr heat-treatment in oxygen at temperatures to 1000 °C showed no volumetric changes and no evidence of a crystalline oxide phase. However, after heat treatment at 1200 and 1400 °C, both materials indicated formation of crystalline silica at their outer surfaces as well as an increase in volume percent up to 2 percent.

(4) Microstructural Analysis

For microstructural analysis, the composite specimens were sectioned normal to the fibers in 6 mm intervals from the specimen ends. Each cross section was polished and examined using SEM and EDAX. Examination of successive cross sections of the composites heat treated in oxygen at temperatures beyond 400 °C indicate oxidation of the carbon core extending at

least up to 20 mm from the specimen ends. Representative backscattered electron, and carbon and oxygen elemental x-ray images of the cross sections of the composites in the as-fabricated condition, and after oxygen treatment at 400, 600, 1000, and 1400 °C are shown in Fig. 15. These cross sections were cut at ~25 mm from the specimen end. Figure 15 shows that the carbon-rich surface coating and the carbon core after oxidation treatment at 400 °C and at 1400 °C are stable, but after oxidation treatment at 600 °C and at 1000 °C, the surface coating is partially decoupled from the RBSN matrix. In addition, the oxygen x-ray images of the cross sections of the composites heat treated at 600 and 1000 °C indicate formation of oxide at the interface; a further proof for the oxidation of the carbon-rich coating.

(5) Effect of a Silica Surface Coating Via Flash Oxidation Pretreatment

SiC/RBSN composites were pre-oxidized in an attempt to provide a diffusional barrier coating of silica on their external surfaces. In all cases, the pre-oxidation treatment involved exposing the composite to oxygen at 1500 °C for 30 min. After the preoxidation treatment, the tensile specimens were heat-treated in oxygen at 600 °C for 100 hr and then tested at room temperature, and the TGA specimens were isothermally exposed up to 100 hr in oxygen at 600 °C to determine their oxidation kinetics. Figure 16 shows the oxidation curve at 600 °C for the pre-oxidized composite. For comparison, the oxidation curve that was shown previously in Fig. 13 for the uncoated composite at the same temperature is included in the figure. The results presented in Fig. 16 indicate that the pre-oxidized specimens showed slower weight loss initially than the unoxidized specimens, but after 120 hr of exposure, they reached a value similar to that of unoxidized specimens.

The room temperature tensile strength data are tabulated in Table III for the as-fabricated, pre-oxidized, and pre-oxidized and oxygen treated specimens at 600 °C for 100 hr. Table III shows that the composites after pre-oxidation

treatment exhibit strength values similar to the as-fabricated composites, but the pre-oxidized composites after 100 hr exposure at 600 °C in oxygen showed strength degradation.

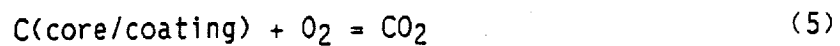
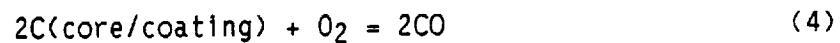
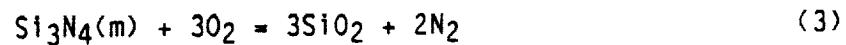
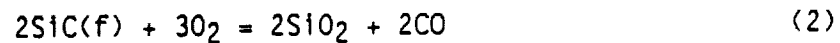
IV. DISCUSSION

The results of this investigation have clearly demonstrated that SiC/RBSN composites after heat treatment in a nitrogen environment at temperatures to 1400 °C for 100 hr showed no loss in mechanical properties when compared with that for the composites in the as-fabricated condition. However, the composites after heat treatment in an oxygen environment beyond 400 °C showed degradation in nearly all properties. The fact that degradation occurred only in an oxidizing environment implies that it is related to oxidation of the composite constituents. In general, the mechanisms of oxidation in multiphase composites are quite complex and those responsible for property degradation may vary depending on the temperature of exposure and the environment. However for SiC/RBSN, it is possible to postulate the mechanisms for mechanical property degradation by understanding the physical effects of oxidation on composite microstructure. This understanding can be achieved by first analyzing the oxidation behavior of the RBSN matrix, the SCS-6 SiC fiber, and the fiber/matrix interfacial bonding.

(1) Oxidation Effects on Composite Constituents

As described earlier, the SiC/RBSN composite is composed of carbon coated silicon carbide fibers in a relatively porous silicon nitride matrix. The SiC fibers themselves have a complex microstructure and consist of a pyrolytic graphite coated carbon core, a SiC sheath, and carbon-rich surface coating which is essentially a mixture of graphite carbon and fine SiC particles.¹⁰ The RBSN matrix contains nearly 30 vol % porosity - most of which is interconnected - and a small amount of residual unreacted silicon (<6 percent).

In an oxidizing environment at high temperatures, the oxygen gas can easily permeate through the porous RBSN matrix and react with the fiber/matrix interface or the RBSN matrix. In addition, because of exposed specimen ends, oxygen can react with the carbon core. Therefore, based on the components of the SiC/RBSN composites, one can propose the following oxidation reactions.



Here the letters *f* and *m* within the brackets refer to the fiber and the matrix, respectively.

The oxidation reactions for SiC and Si₃N₄, Eqs. 2 and 3, involve the consumption of oxygen and release of carbon monoxide or nitrogen. Progression of these reactions requires inward diffusion of oxygen and outward diffusion of gaseous reaction products through a growing oxide scale. The oxidation of silicon is similar to that of SiC or Si₃N₄ and results in growth of silica. In general, when an adherent and tenacious oxide scale grows on the exposed surfaces, the material gains weight. In contrast, oxidation of the carbon-rich surface coating and the carbon core releases gaseous products which when swept away by the carrier gas results in weight loss. The kinetics and temperature ranges of the five reactions (Eqs. (2) to (6) are well known and thus can be used with the oxidation curves of the RBSN matrix and the fibers to understand the underlying oxidation mechanisms.

The oxidation curves for unreinforced RBSN generally showed two or three regions (cf Fig. 13). In the first stage, a small but reproducible weight loss, typically less than 0.25 percent, was observed. This weight loss can be attributed to desorption of moisture from the porous RBSN matrix because equal

amounts of weight gain were measured when dried RBSN specimens were exposed to ambient air. In the second stage of oxidation, net weight increased with exposure time and the rate of weight gain was fairly high. For a set exposure time, the net weight gain increased with increasing temperature. This region was prominent in the oxidation curve at 1000 °C. EDAX analysis of the oxidized specimen at this temperature showed oxide growth both on the outer surfaces as well as at internal porous regions. These observations are consistent with the previously reported results for RBSN.^{11,12} In the third stage of oxidation, especially in the oxidation curves at 1200 and 1400 °C, the rate of weight gain slowed considerably. The reduced oxidation rate in this stage can be attributed to formation of an oxide diffusion barrier coating at the external surfaces. This is supported by the volumetric expansion and XRD results.

The influence of residual silicon on the oxidation behavior of the RBSN matrix is not well established. It is presumed that free silicon oxidizes and forms silica in a similar manner as the RBSN.

If we consider that weight gain is caused by the growth of oxide scales, then we could conclude that the rate of growth of oxide scale and the oxidation of RBSN are insignificant below 800 °C. This is consistent with the general oxidation behavior of silicon based materials. The implication of this finding is that degradation of the composites properties in the temperature range from 600 to 800 °C is probably unrelated to the oxidation of the RBSN matrix.

On the other hand, individual SCS-6 fibers after 100 hr heat treatment in oxygen in the temperature range of 400 to 1200 °C indicated weight loss (Fig. 10). Among the five oxidation reactions previously shown, the only ones that could result in weight loss are the oxidation of the fiber surface

coating and the carbon core (Eqs.(4) and (5)). The rate and extent to which these two reactions proceed at temperatures beyond 400 °C cannot be predicted because of the nonuniform oxidation nature of the core as well as the coating. Based on a density value of 3.17 g/cc for the SiC sheath and 3.07 g/cc for SiC fiber,⁹ and knowledge of the respective volume fraction of the core, sheath and surface coating, the density of the core and the surface coating were calculated from the rule of mixtures. Based on a calculated density value of 2.4 g/cc, a maximum weight loss of 12 percent was estimated. In reality, a maximum weight loss of 7 percent was observed for the fibers after 100 hr heat treatment at 900 °C in oxygen. This indicates either that complete oxidation of the carbon coating and carbon core did not occur, or that other oxidation reactions which resulted in weight gain occurred simultaneously. The growth of silica within the carbon rich surface coating of the heat treated fibers at temperatures beyond 400 °C (cf Fig. 12) suggests that in addition to these two reactions that result in weight loss, namely, the oxidation of the carbon-rich coating and the carbon core, SiC particles within the surface coating are also oxidized. As described earlier, this last reaction results in weight gain. From this we conclude that the net weight change in heat-treated fibers depends on the extent to which these three reactions proceed. The weight change data shown in Fig. 10 suggests that at temperature less than 900 °C, the two weight loss reactions dominate, whereas beyond 900 °C, the weight gain reaction is controlling.

The oxidation of the fiber's surface coating and perhaps the carbon core also resulted in loss of tensile strength of the fibers. The retained strength of fibers after heat treatment depended on the temperature exposure; the higher the exposure temperature, the lower was the retained strength. Since the strength of SiC fibers is controlled by the largest flaws, one could

postulate that strength loss is due to generation of new flaw populations at the surface or in the interior regions of the fibers. Because of the difficulty in retaining the primary fracture surfaces of the heat treated fibers, we were unable to identify the nature and location of the strength limiting flaws. Nevertheless, some insight on flaw location was obtained from the results of flexural strength test fibers. Such tests are primarily sensitive to surface flaws. The room temperature flexural strength measurements on heat treated fibers showed strength loss in the temperature range where tensile strength loss was observed. This indicates that tensile strength degradation of the fibers is primarily due to creation of surface flaws, that is, oxidation of the fiber surface coating.

(2) Oxidation Behavior of Composites

Based on the oxidation curves for the RBSN matrix and the SiC fibers, one can thus explain the oxidation behavior and suggest probable mechanisms for the strength degradation of composites after long time heat treatment in oxygen at temperatures to 1400 °C. In the temperature range 25 to 400 °C, where oxidation of both carbon and Si_3N_4 is kinetically slow, heat treatment of SiC/RBSN composites in oxygen had no effect on their physical and mechanical properties because oxygen did not attack the fiber/matrix interface, the fiber, or the matrix. In the temperature range from 500 to 800 °C, where the oxidation the rate of Si_3N_4 is insignificant, oxygen diffusing through the porous RBSN can react with the fiber-matrix interface and oxidize the carbon-rich coating consisting of carbon and silicon carbide particulates. In addition, oxygen can oxidize the carbon core from the exposed ends of the composite specimens. The reaction products of both these reactions are gases and can escape from the body of the material. The results in weight loss. The rate and extent of weight loss depends on the exposure

temperature and time, and the local conditions established by the reactants and the products. The weight loss observed in the initial stages of oxidation of the composites is attributed to these reactions and levels off as the coating and core are consumed. Moreover, the oxidation of the carbon and SiC particulate also creates voids and porous silica at the fiber/matrix interface, and thus is probably responsible for the loss of those mechanical properties of composites which are dependent of fiber-matrix load transfer.

At 1000 °C, besides oxidation of the carbon core and carbon rich coating, oxidation of the Si₃N₄ material also occurs. The RBSN being a porous material, there is equal probability for oxidation product to grow at internal and external surfaces until inter-connected pores are closed. Unimpeded growth of oxide results in a weight gain region.

At 1200° and 1400 °C, due to the rapid growth of an external protective oxide film, the surface porosity is quickly sealed off and oxidation is restricted to geometrical surfaces, and oxidation of internal pores is limited by the diffusion of oxygen through the oxide scale. This oxide scale was identified to be cristobalite. The formation of cristobalite at these temperatures indicates that the oxide formed reacts with the impurities and the nitriding additives to form a low melting silicate. The formation of a diffusional barrier coating also reduces the oxidation of the interface region between the fiber and the matrix, thus allowing the composite to retain adequate bonding between the fiber and matrix.

The fact that the silica layer formed at high temperatures seals off the surface porosity and retards the diffusion of oxygen inwards suggests that one could use this technique to reduce the oxidation of the fiber/matrix interface at intermediate temperatures. This technique has been effectively used in monolithic RBSN to avoid its vulnerability for internal oxidation in the

temperature range from 0 to 1000 °C.¹¹⁻¹³ In this temperature range oxidizing gas diffuses through the porous RBSN matrix and reacts with it to form silica. On cooling, the internally formed silica produces residual stresses and cracks in the material that lead to losses in properties.⁴⁻¹⁵ In this study, we found that flash oxidation to form a silica coating on the composite surfaces is ineffective in reducing diffusion of oxygen in the intermediate temperature range from 600 to 1000°. During cool down from the flash coating temperature, the silica surface coating apparently cracked, allowing fiber surface attack during 100 hr exposure at 600 °C.

(3) Mechanisms for Composite Mechanical Degradation

In general, the mechanical performance of a fiber reinforced composite is controlled by the interfacial shear strength, and the elastic and fracture properties of the constituents. However the specific factors that affect the three mechanical properties, namely the elastic modulus, the first matrix cracking strength, and the ultimate tensile strength, are different. Thus each property should be examined separately in order to interpret possible oxidation mechanisms.

(a) Primary elastic modulus. The primary elastic modulus, E_c , along the fiber direction for a unidirectionally reinforced composite depends upon the constitutive moduli and volume fractions, and the nature of bonding between the fiber and matrix. For adequately bonded composites, the elastic modulus can be estimated from the rule of mixtures:

$$E_c = E_f V_f + E_m V_m \quad (7)$$

Here E is elastic modulus and V is volume fraction, and the subscripts c , f , and m refer to composite, fiber, and matrix, respectively. On the other hand, for a totally unbonded composite, that is $E_f = 0$, Eq. (7) reduces to

$$E_c = E_m V_m \quad (8)$$

Substituting the values of $E_f = 400$ GPa, $E_m = 110$ GPa, $V_m = 0.7$, and $V_f = 0.3$ in Eqs. (7) and (8), one calculates $E_c = 197$ GPa for well bonded composites and $E_c = 77$ GPa for unbonded composites. The primary elastic modulus values for SiC/RBSN composites in the as-fabricated condition and after oxidation treatment at 1200 and 1400 °C were similar and agreed well with the predicted value of 197 GPa. This means that bonding between the fiber and the matrix is adequate. On the other hand, the elastic modulus values for the composites exposed to oxygen in the temperature range from 600 to 1000 °C were higher than that for the totally unbonded case but lower than the adequately bonded case: an indication of partial loss of bonding between fiber and matrix.

(b) First matrix cracking stress. The first matrix cracking stress is a difficult property to estimate from constituent properties. Nonetheless, composite theories^{8,16,17} that are based on fracture mechanics concepts have shown that the first matrix cracking stress in uniaxially reinforced composites varies with interfacial shear strength, the elastic properties of the components, and the fracture toughness/fracture surface energy of the matrix. Although their applicability for SiC/RBSN composites is not fully established, these theories predict loss of the first matrix cracking stress/strain with decrease in interfacial shear strength, assuming that the elastic properties of the constituents are unaffected. Indeed this behavior was observed for the SiC/RBSN composites heat treated in oxygen in the temperature range from 600 to 1000 °C. In addition, a good correlation was seen between the first matrix cracking stress and the primary composite modulus since the strain to matrix fracture remained nearly the same (Table II).

(c) The ultimate tensile strength. The ultimate tensile strength of a unidirectionally reinforced composite, σ_{uts} , is strongly influenced by the fibers and can be estimated from the equation.¹⁸

$$\sigma_{uts} = \sigma_f^B V_f \quad (9)$$

where σ_f^B is the bundle strength of fibers measured at gauge length, l , and V_f is the volume fraction of fibers.

The bundle strength is also related to the average tensile strength of the fiber, σ , measured at gauge length, l , by the equation.¹⁸

$$\sigma_f^B / \sigma = (me)^{-1/m} / \Gamma[(m+1)/m] \quad (10)$$

Where Γ is the gamma function and m is the Weibull modulus.

In fiber reinforced ceramic composites extraction of fibers from the matrix poses problems because the solvents used for dissolving the matrix also attack the fibers. However, if we assume that between 600 to 1000 °C, the degradation in the average tensile strength of individual SiC fibers that were heat treated is similar to that of the fibers in the composite, then the degradation behavior of ultimate tensile strength for the composite can be estimated. This assumption is valid because in the intermediate temperature range the oxidizing gases can easily permeate through the composite and can react with the fibers as they would with individual SiC fibers exposed to the same environment.

Since degradation of the composite ultimate tensile strength is correlated with that of the fiber average tensile strength, we conclude that the loss in composite strength was due to fiber degradation. Indication of fiber degradation is seen in Figs. 11 and 13.

The above analysis has shown that loss of mechanical properties of the composites is due to loss of bonding between the fiber and matrix and to fiber degradation. The basic mechanism by which interface and fiber degradation

occurs can be attributed to oxidation of the carbon-rich surface coating on SCS-6 SiC fiber. Further proof for this mechanism comes from the microstructural studies which clearly showed a correlation between the stability of the carbon-rich coating and retained mechanical properties. Based on this model and the oxidation behavior of the matrix, the mechanical property degradation seen in composites after exposure to oxidizing environments can thus be summarized.

In the temperature range from 25 to 400 °C, where oxidation of the carbon is kinetically slow, long term exposure of SiC/RBSN composites in an oxidizing environment has no degrading influence on mechanical properties. In contrast, in the temperature range from 600 to 1000 °C, where internal oxidation of RBSN and oxidation of carbon is more likely, oxidation of the carbon-rich surface coating causes loss of bonding between the fiber and matrix and fiber strength loss, which in turn affects the three key composite mechanical properties. The extent to which the mechanical property degradation occurs depends on the amount of the coating oxidized and the loss in the load transfer characteristics. In the temperature range from 1200 to 1400 °C rapid growth of the oxide at the initial stages of oxidation exposure limits inward diffusion of oxygen and oxidation of the fiber coating. This permits the materials to retain a greater part of its as-fabricated properties.

V. SUMMARY OF RESULTS

The room temperature mechanical properties of SiC/RBSN composites after 100 hr exposure in nitrogen and in oxygen environments at temperature to 1400 °C have been measured. The major findings are as follows;

(A) SiC/RBSN matrix composites retained their as-fabricated mechanical properties after nitrogen exposure at temperature to 1400 °C.

In contrast, composites after oxygen exposure in the temperature range of 600 to 1000 °C showed loss in all the mechanical properties measured; whereas composites exposed in temperature range of 1200 to 1400 °C retained a greater part of their mechanical properties.

(B) Based on the TGA and microstructural characterization results, several oxidation mechanisms that may affect the mechanical properties of the composites have been identified. However the dominant mechanism is identified as oxidation of the fiber surface coating. In the temperature range of 600 to 1000 °C, oxidation of the fiber surface coating promotes debonding of the fiber from the RBSN matrix as well as fiber strength degradation. Both these factors are responsible for the composite property degradation. In contrast, in the temperature range of 1200 to 1400 °C the oxidation of the fiber surface coating is minimized by the growth of oxide diffusion barrier coating at the external surfaces of the composite. This improved the oxidative stability of the composites.

(C) A silica layer intentionally grown on composite external surfaces by a flash oxidation technique did not serve as an effective barrier coating in avoiding the harmful effects of oxygen diffusion in the intermediate temperature range from 600 to 1000 °C on the mechanical properties of the SiC/RBSN composites.

VI. CONCLUSIONS

The results of this investigation have clearly shown that the mechanical performance of SiC/RBSN composites depends on the oxidative stability of the fiber surface coating and the load transfer characteristics between the fiber and the matrix. In the temperature range where oxidation of carbon is kinetically feasible or diffusion of oxygen through the porous matrix is limited by diffusional barrier surface oxide coating, the composites after long term exposure in an oxidizing environment retain a greater fraction of

their properties in the as-fabricated condition. In the temperature range where oxygen attacks the fiber surface coating, the composite displayed poor mechanical performance. Thus, it can be concluded that the long term oxidative stability and the mechanical performance for the composite at intermediate temperatures, i.e., between 600° and 1000 °C, can be improved by providing an effective barrier to oxygen attack of the carbon-rich fiber coating. Possible approaches for accomplishing this are by the addition of an oxidation resistant surface coating on SCS-6 SiC fibers or by sealing off the surface porosity with a dense, impervious layer of SiC or Si₃N₄, or by fully densifying the Si₃N₄ matrix.

REFERENCES

1. A. Briggs and R.W. Davidge, "Fabrication, Properties and Applications of Borosilicate Glass Reinforced with Continuous Silicon Carbide Fibers," pp. 153-164 in Whisker and Fiber-Toughened Ceramics. Edited by R.A. Bradly, D.E. Clark, D.C. Larsen and J.O. Stiegler. ASM International, 1988.
2. J.J. Brennan and K.M. Prewo, "Silicon Carbide Fiber Reinforced Glass-Ceramic Matrix Composites Exhibiting High Strength and Toughness," J. Mater. Sci., 17 [8] 2371-2383 (1982).
3. L. Heraud, and P. Spriel, "High Toughness C-SiC and SiC-SiC Composites in Heat Engines," pp. 217-224 in Whisker and Fiber-Toughened Ceramics. Edited by R.A. Bradly, D.E. Clark, D.C. Larsen and J.O. Stiegler. ASM International, 1988.
4. C.A. Andersson, P. Borron-Antolin, A.S. Fareed, and G.H. Schiroky, "Properties of Fiber-Reinforced Lanthanide Alumina Matrix Composites," pp. 209-216 in Whisker and Fiber-Toughened Ceramics. Edited by R.A. Bradly, D.E. Clark, D.C. Larsen, and J.O. Stiegler. ASM International, 1988.

5. R.T. Bhatt, "The Properties of Silicon Carbide Fiber Reinforced Silicon Nitride Composites," pp. 199-208 in Whisker and Fiber-Toughened Ceramics. Edited by R.A. Bradley, D.E. Clark, D.C. Larsen and J.O. Stiegler. ASM International, 1988.
6. N.D. Corbin, G.A. Rosetti Jr., and S.D. Hartline, "Microstructure/Property Relationships for SiC Filament-Reinforced RBSN--Reaction-Bonded Silicon Nitride," Ceram. Eng. Sci. Proc., 7 [7-8] 958-968 (1986).
7. R.T. Bhatt, "Method of Preparing Fiber Reinforced Ceramic Materials," U.S. Pat. No. 4689188, 1987.
8. J. Aveston, G.A. Cooper, and A. Kelley, "Single and Multiple Fracture," pp. 15-26 in The Properties of Fiber Composites, Proceedings of the Conference. IPC Science and Technology Press Ltd., Surrey, England, 1971.
9. J.A. Dicarlo and W. Williams, "Dynamic Modulus and Damping of Boron, Silicon Carbide and Alumina Fibers," NASA TM-81422, Jan. 1980.
10. P. Pirouz, G. Morscher, and J. Chung, "Surfaces and Interfaces of Ceramic Materials," to be published in the Proceeding of NATO Advanced Study Institute conference, Kluwers Academic Publishers, Dordrecht, Netherlands, 1989.
11. D.W. Richardson, "Modern Ceramic Engineering: Properties, Processing and Use in Design." Marcel Dekker, Inc. New York, 1982.
12. L.J. Lindberg, D.W. Richerson, W.D. Carruthers, and H.M. Gersch, "Oxidation Stability of Advanced Reaction-Bonded Si₃N₄ Materials," Am. Ceram. Soc. Bull., 61 [5] 574-578 (1982).
13. O.J. Gregory and M.H. Richman, "Thermal Oxidation of Sputter-Coated Reaction-Bonded Silicon Nitride," J. Am. Ceram. Soc., 67 [5] 335-340 (1984).

14. R.W. Davidge, A.G. Evans, D. Gilling, and P.R. Wilyman, "Oxidation of Reaction-Sintered Silicon Nitride and Effect on Strength," pp. 321-343 in *Special Ceramics 5*. Edited by P. Popper, British Ceramic Association, Stoke-on-Trent, 1972.
15. A.G. Evans and R.W. Davidge, "The Strength and Oxidation of Reaction-Sintered Silicon Nitride," J. Mater. Sci., 5 [1] 314-325 (1970).
16. D.B. Marshall, B.N. Cox, and A.G. Evans, "The Mechanics of Matrix Cracking in Brittle-Matrix Fiber Composites," Acta Metall., 33 [11], 2013-2021 (1985).
17. B. Budiansky, J.W. Hutchinson, and A.G. Evans., "Matrix Fracture in Fiber-Reinforced Ceramics," J. Mech. Phys. 34 [2], 167-189 (1986).
18. H.T. Corten, "Micromechanics and Fracture Behavior of Composites," pp. 27-105 in *Modern Composite Materials*. Edited by L.J. Broutman and R.H. Krock. Addison-Wesley, New York, 1967.

TABLE I. - ROOM TEMPERATURE PHYSICAL AND MECHANICAL PROPERTY DATA
FOR UNIDIRECTIONALLY REINFORCED SiC/RBSN COMPOSITES

Fiber fraction, percent	28±2
Density, gm/cc	2.3±0.1
Porosity, percent	30±5
Pore size, μm	<0.03
Elastic modulus, GPa	193±7
Tensile strength, MPa	
Matrix fracture stress	227±40
Ultimate strength	682±150

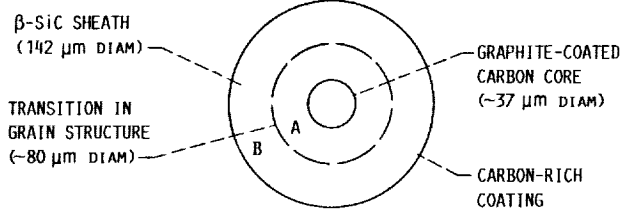
TABLE II. - MATRIX FRACTURE PROPERTIES FOR SiC/RBSN COMPOSITES
[V_f ~ 0.3.]

Condition	First matrix cracking stress, MPa	First matrix cracking strain, percent	Average matrix crack spacing, mm
As fabricated	227±40	0.12	0.8±0.2
After 100-hr heat treatment in oxygen at-			
400°	220±20	0.12	0.75±0.2
600°	154±30	0.11	12±2
800°	136±20	0.09	12±3
1000°	130±20	0.09	10±4

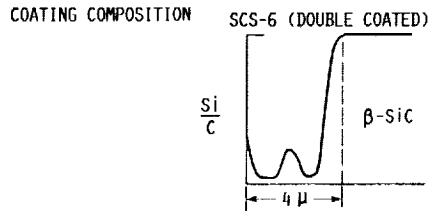
TABLE III. - ROOM TEMPERATURE MECHANICAL PROPERTIES FOR
AS-FABRICATED AND FLASH OXIDATION COATED
SiC/RBSN COMPOSITES

Condition	Matrix fracture stress, MPa	Ultimate composite strength, MPa
As-fabricated	227±40	682±150
Flash coated ^a	210	675
Flash coated ^a and then treated at 600°C for 100 hr	100	127

^aFlash coated at 1500 °C for 30 min in oxygen.



(a) SCHEMATIC OF CROSS SECTION OF FIBER.



(b) COMPOSITION PROFILE OF CARBON-RICH COATING ON FIBER SURFACE (TEXTRON SCS-6).

FIGURE 1. - DETAILS OF CVD SiC FIBER.

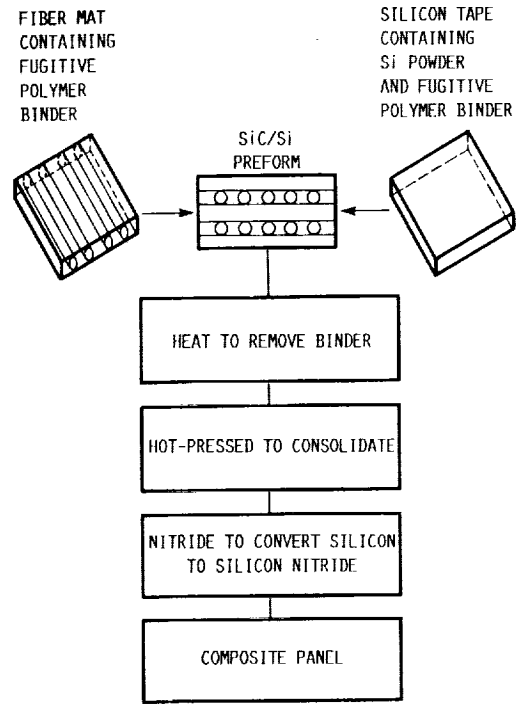


FIGURE 2. - BLOCK DIAGRAM SHOWING THE SiC/RBSN COMPOSITE FABRICATION PROCESS.

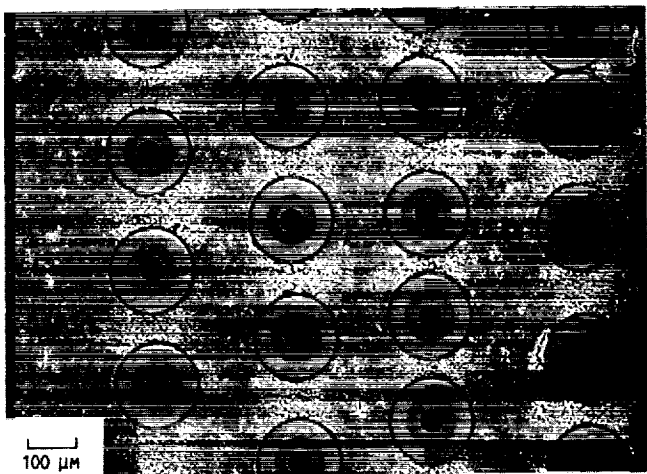


FIGURE 3. - TYPICAL CROSS SECTION OF 30 VOL % SiC/RBSN COMPOSITE SHOWING FIBER DISTRIBUTION AND MATRIX POROSITY.

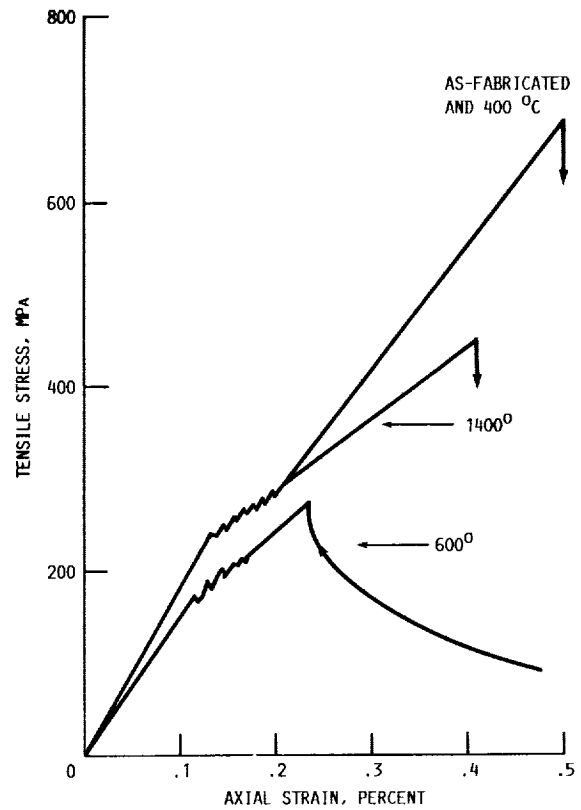


FIGURE 4. - ROOM TEMPERATURE STRESS-STRAIN CURVES FOR SiC/RBSN COMPOSITES IN AS-FABRICATED AND AFTER 100 HR HEAT-TREATMENT IN OXYGEN AT 400°, 600° AND 1400 °C.

ORIGINAL PAGE
BLACK AND WHITE PHOTOGRAPH

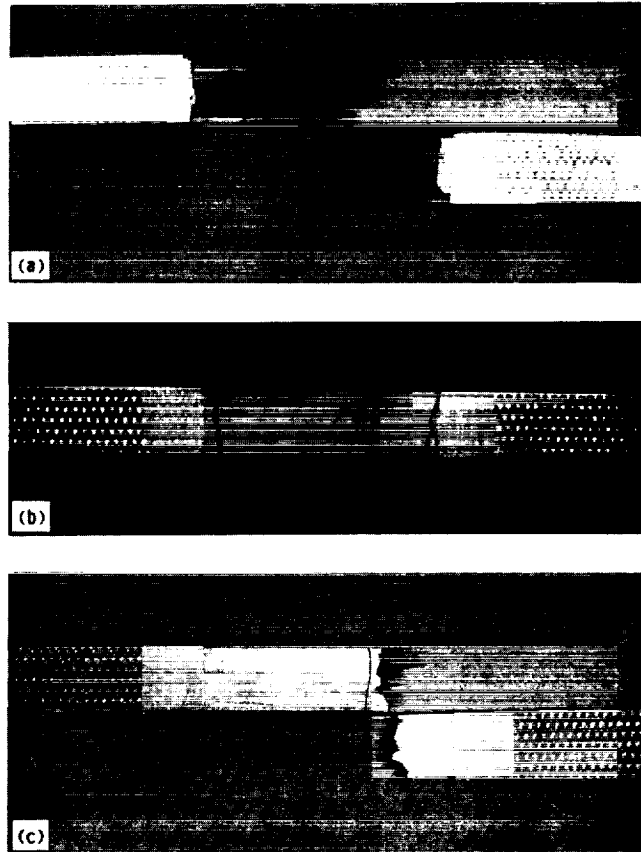


FIGURE 5. - ROOM TEMPERATURE TENSILE FRACTURED SPECIMENS OF SiC/RBSN COMPOSITES (a) AS-FABRICATED CONDITION (b), AND (c) AFTER 100 HR HEAT-TREATMENT IN OXYGEN AT 600° AND 1400 °C, RESPECTIVELY.

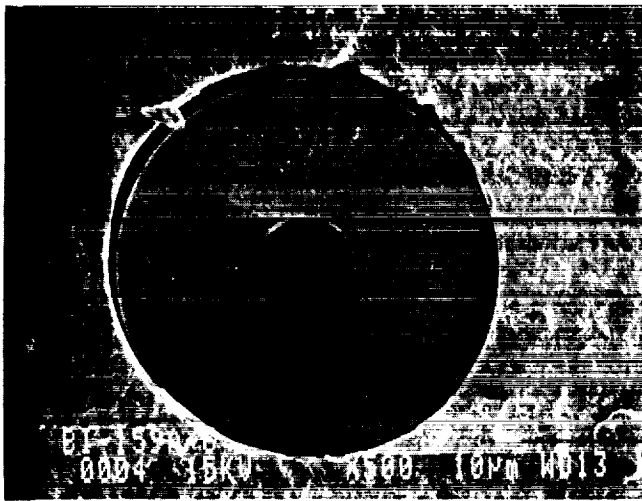


FIGURE 6. - SEM PHOTOGRAPH OF A TYPICAL TENSILE FRACTURE SURFACE OF A SiC/RBSN COMPOSITE AFTER 100 HR HEAT-TREATMENT IN OXYGEN 1000 °C SHOWING DEBONDING OF FIBER COATING AND VOIDS AT FIBER/MATRIX INTERFACIAL REGION.

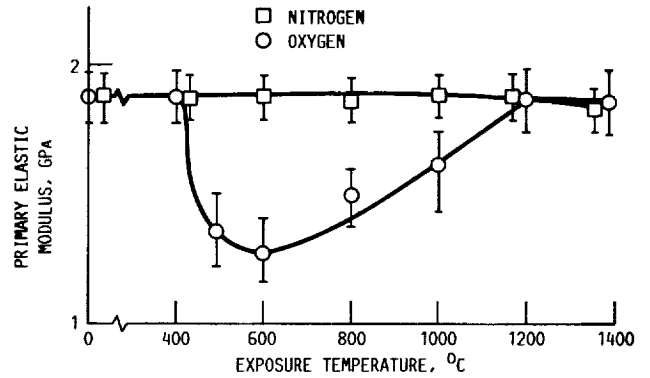


FIGURE 7. - PRIMARY ELASTIC MODULUS OF SiC/RBSN COMPOSITES AT ROOM TEMPERATURE AFTER 100 HR HEAT TREATMENT IN NITROGEN AND IN OXYGEN AT THE INDICATED TEMPERATURES.

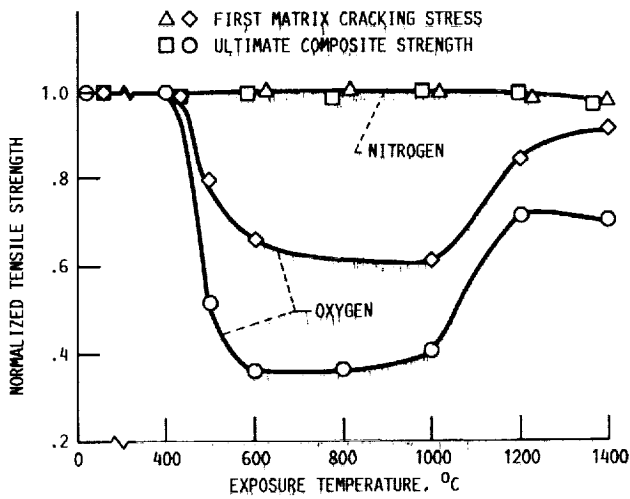


FIGURE 8. - MATRIX CRACKING STRESS AND ULTIMATE COMPOSITE STRENGTH OF SiC/RBSN COMPOSITES AT ROOM TEMPERATURE AFTER 100 HR HEAT-TREATMENT IN NITROGEN AND IN OXYGEN AT THE INDICATED TEMPERATURES.

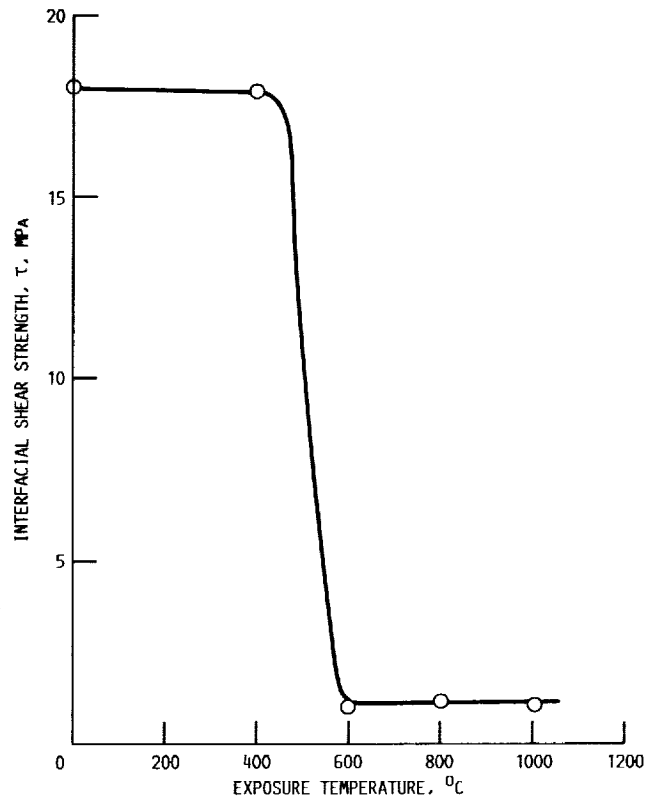


FIGURE 9. - INTERFACIAL SHEAR STRENGTH OF SiC/RBSN COMPOSITES AT ROOM TEMPERATURE AFTER 100 HR HEAT-TREATMENT IN OXYGEN AT THE INDICATED TEMPERATURES.

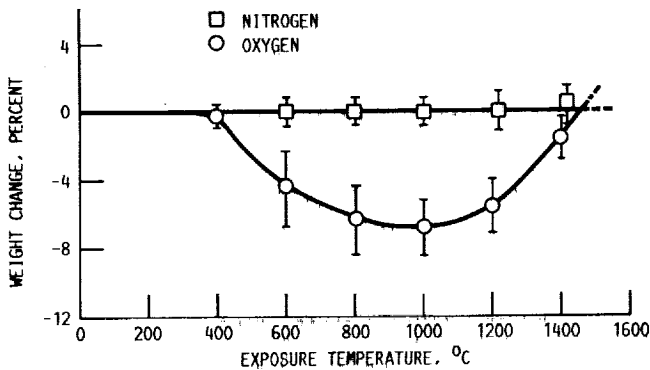


FIGURE 10. - WEIGHT CHANGE OBSERVED IN DOUBLE COATED SCS-6 SiC FIBERS AFTER 100 HR HEAT TREATMENT IN NITROGEN AND IN OXYGEN IN THE TEMPERATURE RANGE OF 400^o-1400 °C.

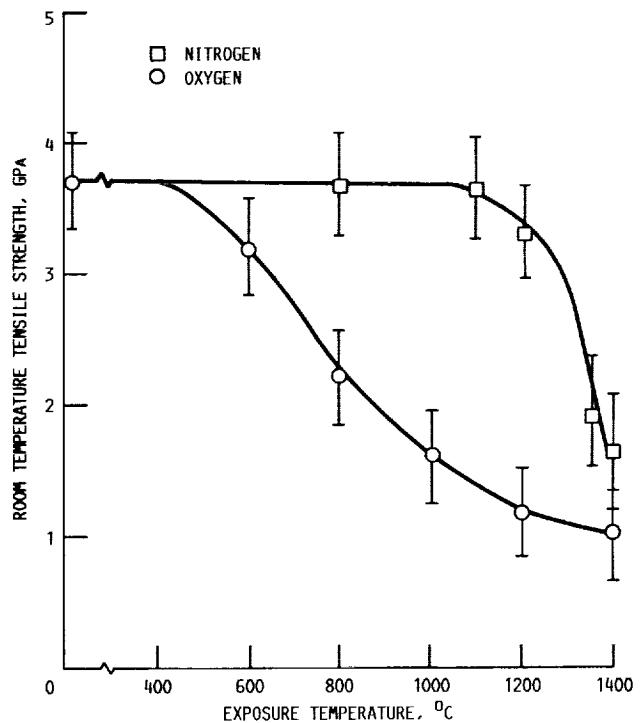


FIGURE 11. - ROOM TEMPERATURE TENSILE STRENGTH OF DOUBLE COATED SCS-6 SiC FIBERS AFTER 100 HR HEAT TREATMENT IN NITROGEN AND IN OXYGEN AT THE INDICATED TEMPERATURES.

ORIGINAL PAGE
BLACK AND WHITE PHOTOGRAPH

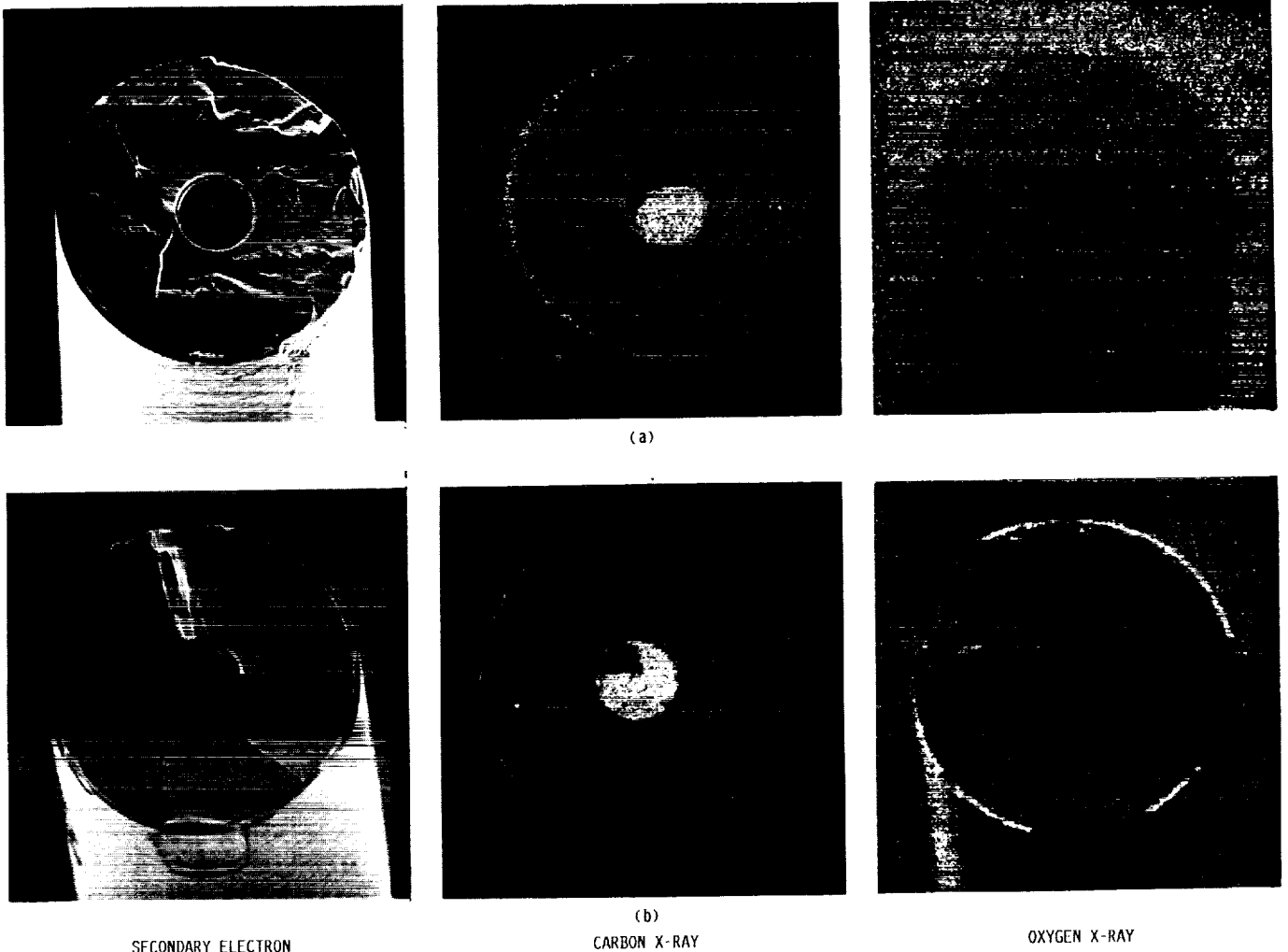


FIGURE 12. - SEM MICROGRAPHS AND ELEMENTAL X-RAY IMAGES FOR FRACTURED SCS-6 SiC FIBERS (a) AS-FABRICATED, (b) AFTER 100 HR EXPOSURE IN OXYGEN AT 600 °C.

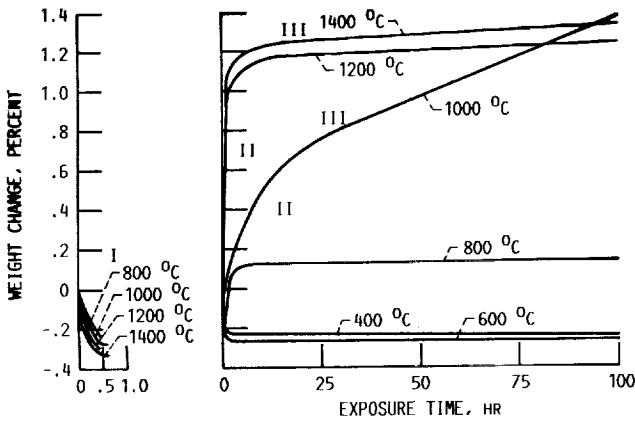


FIGURE 13. - OXIDATION BEHAVIOR FOR UNREINFORCED RBSN UP TO 100 HR EXPOSURE IN FLOWING OXYGEN AT INDICATED TEMPERATURES.

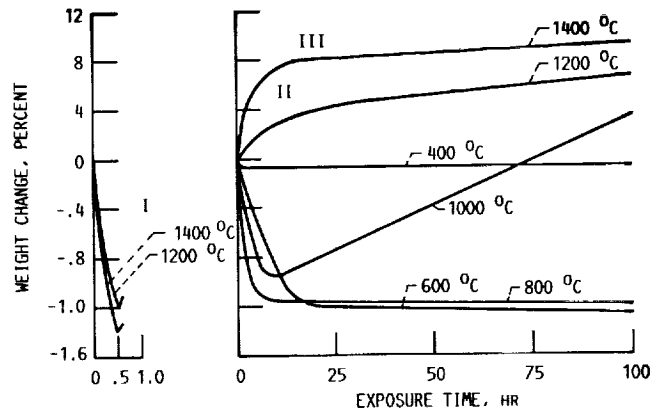
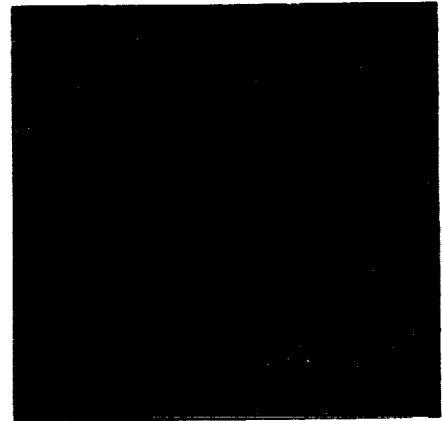
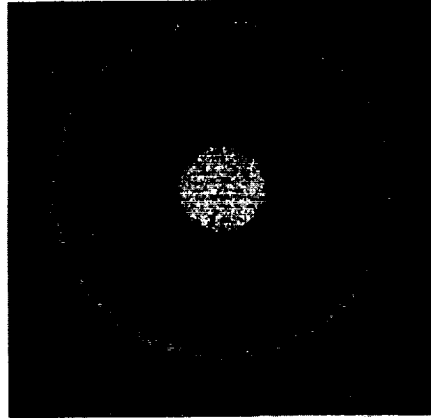
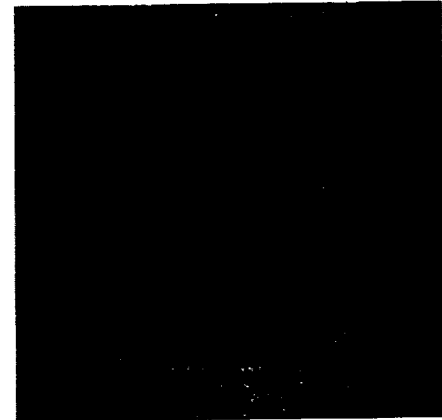
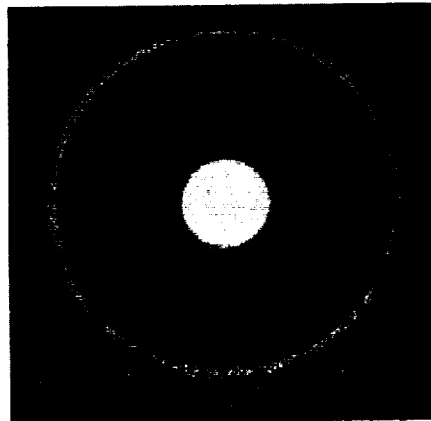
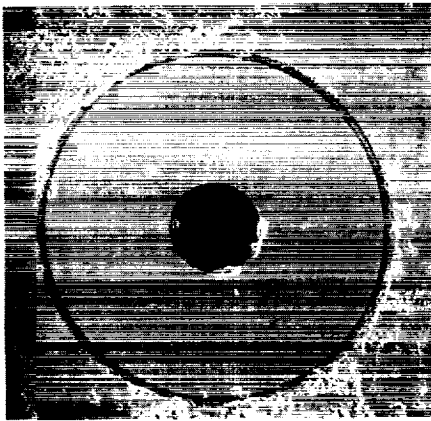


FIGURE 14. - OXIDATION BEHAVIOR FOR SiC/RBSN COMPOSITES UP TO 100 HR EXPOSURE IN FLOWING OXYGEN AT THE INDICATED TEMPERATURES.



AS-FABRICATED



BACK SCATTER

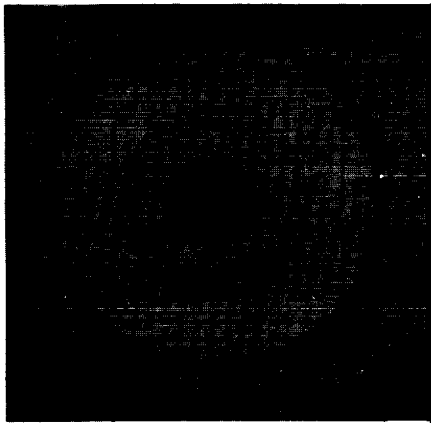
400 °C
CARBON X-RAY

OXYGEN X-RAY

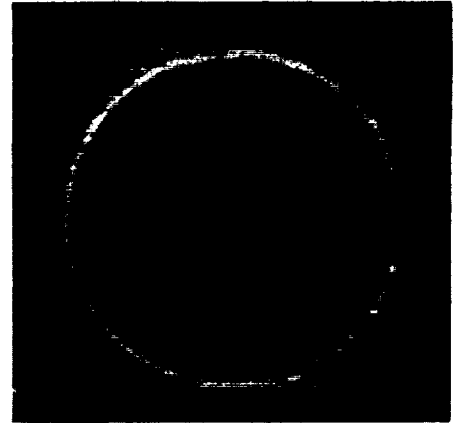
FIGURE 15. - SEM MICROGRAPH AND ELEMENTAL X-RAY IMAGES FOR SiC/RBSN COMPOSITES IN THE AS-FABRICATED CONDITION AND AFTER 100 HR HEAT-TREATMENT IN OXYGEN AT THE INDICATED TEMPERATURES.

ORIGINAL PAGE
BLACK AND WHITE PHOTOGRAPH

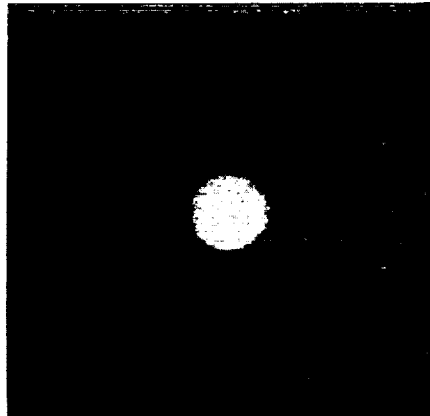
ORIGINAL PAGE
BLACK AND WHITE PHOTOGRAPH



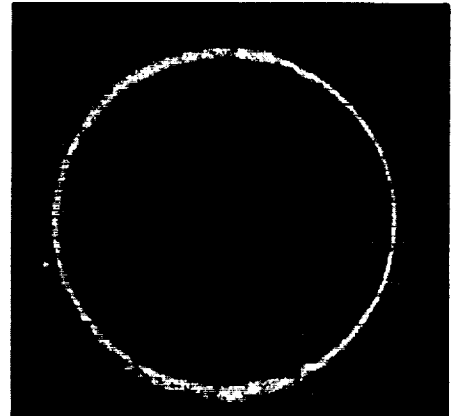
600 °C



BACK SCATTER

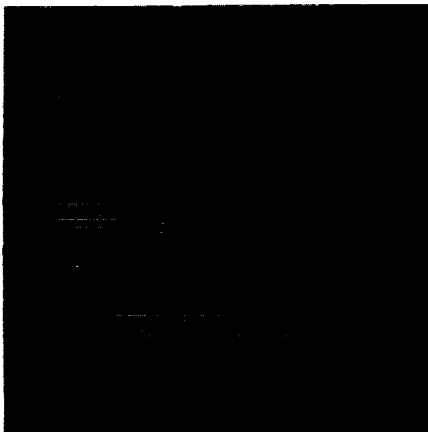


1000 °C
CARBON X-RAY

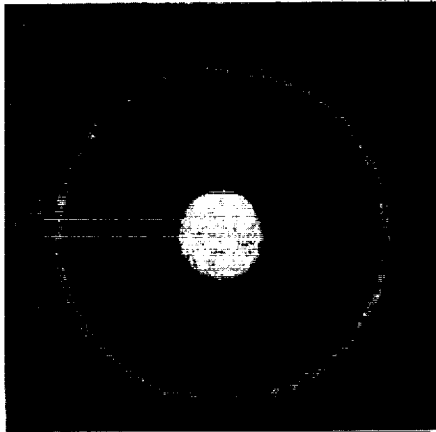


OXYGEN X-RAY

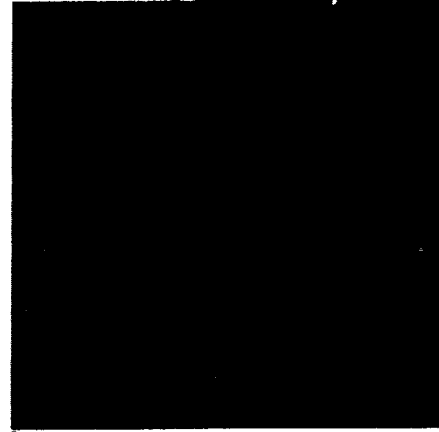
FIGURE 15. - CONTINUED.



BACK SCATTER



1400 °C
CARBON X-RAY



OXYGEN X-RAY

FIGURE 15. - CONCLUDED.

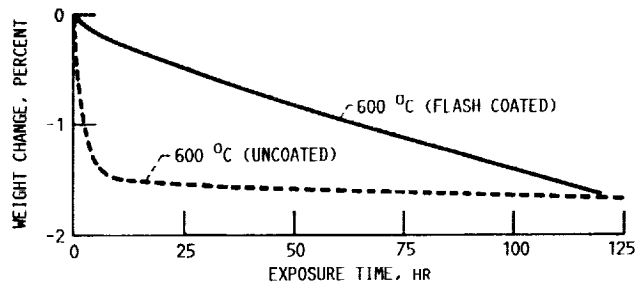


FIGURE 16. - OXIDATION BEHAVIOR OF FLASH COATED (SILICA) SIC/RBSN COMPOSITE AT 600 °C.

ORIGINAL PAGE
BLACK AND WHITE PHOTOGRAPH

1. Report No. NASA TM-102360 AVSCOM TR 89-C-018		2. Government Accession No.		3. Recipient's Catalog No.	
4. Title and Subtitle Oxidation Effects on the Mechanical Properties of SiC Fiber-Reinforced Reaction-Bonded Silicon Nitride Matrix Composites				5. Report Date November 1989	
				6. Performing Organization Code	
7. Author(s) Ramakrishna T. Bhatt				8. Performing Organization Report No. E-5074	
9. Performing Organization Name and Address NASA Lewis Research Center Cleveland, Ohio 44135-3191 and Propulsion Directorate U.S. Army Aviation Research and Technology Activity—AVSCOM Cleveland, Ohio 44135-3127				10. Work Unit No. 510-01-0A	
				11. Contract or Grant No.	
12. Sponsoring Agency Name and Address National Aeronautics and Space Administration Washington, D.C. 20546-0001 and U.S. Army Aviation Systems Command St. Louis, Mo. 63120-1798				13. Type of Report and Period Covered Technical Memorandum	
				14. Sponsoring Agency Code	
15. Supplementary Notes					
16. Abstract The room temperature mechanical properties of SiC fiber-reinforced reaction-bonded silicon nitride composites (SiC/RBSN) were measured after 100 hr exposure at temperatures to 1400 °C in flowing nitrogen and in oxygen environments. The composites consisted of ~30 vol % uniaxially aligned 142 μm diameter SiC fibers (Textron SCS-6) in a reaction-bonded Si ₃ N ₄ matrix. The results indicate that composites heat-treated in a nitrogen environment at temperatures to 1400 °C showed deformation and fracture behavior equivalent to that of the as-fabricated composites. On the other hand, the composites heat-treated in an oxidizing environment beyond 400 °C yielded significantly lower ultimate tensile strength values. Specifically in the temperature range from 600 to 1000 °C, composites retained ~40 percent of their as-fabricated strength, and those heat-treated in the temperature range from 1200° to 1400 °C retained ~70 percent. Nonetheless for all oxygen heat treatment conditions, composite specimens displayed strain capability beyond the matrix fracture stress; a typical behavior of a tough composite. For the oxygen treated composites, the variation of the primary elastic modulus, the first matrix cracking stress, and the interfacial shear strength with heat treating temperature showed trends similar to that of the ultimate tensile strength. Thermogravimetric and microstructural characterization results indicate that the oxygen effects were influenced by two different reactions, namely oxidation of the carbon-rich fiber surface coating and oxidation of the RBSN matrix. The dominant oxidation reaction controlling mechanical behavior depended on the exposure temperature, that is, the carbon reaction occurring from 600° to 1000 °C and the matrix reaction occurring above 1000 °C. Surface coating the composites with a thin layer of silica by a flash oxidation technique appears to have no significant influence on oxidation effects.					
17. Key Words (Suggested by Author(s)) Ceramic composites; Fiber-reinforced oxidation; SiC; Si ₃ N ₄ ; Mechanical properties			18. Distribution Statement Unclassified—Unlimited Subject Category 24		
19. Security Classif. (of this report) Unclassified		20. Security Classif. (of this page) Unclassified		21. No of pages 38	22. Price* A03

